Wang Chao (Orcid ID: 0000-0003-1589-1240)

Wang Bin (Orcid ID: 0000-0002-5726-108X)

Unprecedented Northern Hemisphere tropical cyclone genesis in 2018 shaped by subtropical warming in the North Pacific and the North Atlantic

Chao Wang[1,2], Bin Wang[2,1] and Jian Cao[1]

[1]Key Laboratory of Meteorological Disaster of Ministry of Education, Joint International Research Laboratory of Climate and Environment Change, Collaborative Innovation Center on Forecast and Evaluation of Meteorological Disasters and Earth System Modeling Center, Nanjing University of Information Science and Technology, Nanjing, China

[2]Department of Atmospheric Sciences and International Pacific Research Center, University of Hawaii at Manoa, Honolulu, HI 96822, USA

November 1, 2019

Revised for *Geophysical Research Letters*

Corresponding author:

Bin Wang: wangbin@hawaii.edu

Chao Wang: wangchao.typhoon@gmail.com

Key Points:

1. Northern Hemisphere tropical cyclone genesis frequency in June-September of 2018 reached a record high since 1965.

2. This unprecedented tropical cyclone genesis was mainly driven by the North Pacific and the subtropical North Atlantic.

3. Subtropical ocean warming in the North Pacific and the North Atlantic was responsible for the unprecedented tropical cyclone genesis.

Abstract

Northern Hemisphere tropical cyclone (TC) genesis (TCG) frequency in June-September of 2018 reached a record high since 1965. This unprecedented TCG was mainly driven by the North Pacific (NP) and the subtropical North Atlantic (NA). TCs in the western North Pacific (WNP) predominately took a northward-recurving track, resulting in the highest number of named storm days in the subtropical WNP on record. TCs in the eastern North Pacific propagated anomalously westward with three Category 4-5 hurricanes reaching the central North Pacific. The unprecedented TCG in the NP was caused by a persistent weakening of the NP subtropical high that was tightly coupled with the subtropical NP sea surface temperature (SST) warming. In the NA, enhanced TCG was mainly found in the subtropics owing to a favorable large-scale environment forced by subtropical SST warming. The result here has important implications for understanding variability in TC activity on the hemisphere-scale.

Key words: Tropical cyclone genesis, Northern Hemisphere tropical cyclone season, North Pacific subtropical high, subtropical sea surface warming

Plain Language Summary

The Northern Hemisphere (NH) has about 60 tropical cyclones (TCs) every year, which account for about 70% of the global total and exert significant societal and economic impacts on islands and coastal regions. In 2018, 20% more TCs (i.e. 72 TCs) were observed compared with the long-term average. This active TC genesis (TCG) mainly occurred in June-September over the North Pacific (NP) and the subtropical North Atlantic (NA), resulting in a record high since the satellite era began (1965 onwards). The unprecedented NH TCG was likely driven by subtropical sea surface temperature warming in the NP and the NA and an associated modulation of the large-scale environment important for TCG. These results suggest a crucial role of subtropical sea surface temperature in NH TC activity and thus can provide some instructive implications for understanding changes in TC activity on the hemisphere-scale.

1. Introduction

The Northern Hemisphere (NH) generates about 60 tropical cyclones (TCs) every year, accounting for about two-thirds of global TC genesis (TCG) frequency (Frank & Young, 2007; Gray, 1968; Maue, 2009). In 2018 the NH had 72 named TCs (Fig.1), which is the third-highest TCG frequency since 1965 (figure not shown). Notably, most of the TCs in the western North Pacific (WNP) took a northward-recurving track, with several causing significant impacts in subtropical East Asia. For example, category 5 typhoon Jebi (2018) made landfall over Japan. It was the strongest typhoon to strike Japan since Yancy (1993) and caused significant damage in Japan. In the eastern North Pacific (ENP), the 2018 hurricane season featured the highest Accumulated Cyclone Energy value on record (Wood et al., 2019). Enhanced TC activity and eastward steering flow over the ENP favored TCs propagating westward and reaching the central North Pacific (CNP). Three Category 4-5 hurricanes travelled across the CNP where normally intense TC occurrence is rare (only 0.7 Category 4-5 hurricanes occurred per year on average, Pao Shin Chu & Clark, (1999), Fig. 1).

Previous studies have found that El Niño–Southern Oscillation (ENSO) has profound impacts on TC activity in many individual TC basins (Camargo et al., 2010; Camargo & Sobel, 2005; Chan, 1985; Clark & Chu, 2002; Gray, 1984; Lander, 1994; Singh et al., 2000; B. Wang & Chan, 2002; C. Wang, Wang, et al., 2019a, 2019b; C. Wang & Wang, 2019; Zhao & Wang, 2019). In the WNP, ENSO has an insignificant effect on the total TC genesis number, but the warm phase of ENSO (i.e. El Niño) tends to increase aggregated TC metrics such as named storm days and Accumulated Cyclone Energy by shifting TCG locations southeastward and

allowing for longer tracks over the warm ocean (Camargo & Sobel, 2005; B. Wang & Chan, 2002; C. Wang & Wang, 2019; C. Wang & Wu, 2016). In the central North Pacific (CNP) and ENP, higher TC frequency is found in the developing year of an El Niño (Camargo et al., 2008; P S Chu, 2004; Clark & Chu, 2002; Sobel et al., 2016). Over the North Atlantic (NA), hurricane activity tends to be suppressed in El Niño years, while it tends to be enhanced in La Niña years (Goldenberg & Shapiro, 1996; Gray, 1984; Patricola et al., 2014; Tang & Neelin, 2004).

The summer of 2018 was predominately in an El Niño developing phase. From May to October 2018, the running 3-month mean Oceanic Niño Indices (Niño 3.4 SST anomalies in the equatorial Pacific) were -0.1, 0.1, 0.1, 0.2, 0.4 and 0.7, respectively. Therefore, the Pacific SSTs evolved from La Niña conditions during the previous winter to weak El Niño conditions by October 2018. Nevertheless, the weak El Niño conditions were insufficient to cause the extreme TCG. Therefore, it is unclear why the summer of 2018 produced so many TCs in the NH.

The majority of previous studies have focused on the variability of TC activity in individual TC basins, while less is known about the factors controlling TC activity on the hemisphere-scale. Sobel et al. (2016) found that the NH can experience high levels of TC activity with quasi-El Niño conditions. Maue (2009) suggested that NH TC activity is closely linked to the dominant modes of NP climate variability such as the North Pacific Gyre Oscillation (NPGO). A negative phase of the NPGO occurred in the summer of 2018, which seems to be consistent with the heightened TC activity that the NH experienced in 2018 (Maue, 2009; C. Wang, Wu, et al., 2019; Wei Zhang et al., 2013). But it is unclear how abnormal the

year 2018 is compared to historical records. If it is indeed an exceptional season, what caused it?

2. Data, definition of genesis potential index and numerical model

TC best track data from the National Hurricane Center (NHC, Landsea & Franklin, 2013) for the NA, the ENP and the CNP, and from the Joint Typhoon Warming Center (JTWC, J.-H. Chu et al., 2002) for the WNP and the northern Indian Ocean (NIO) were used to obtain TC information for the period of 1965-2017. Because there is no intensity information provided in the JTWC best tracks for the NIO until 1972, TC counts for 1965-1971 were derived from the electronic Atlas data from the India Meteorological Department (2008). Metrics for the 2018 TC activity such as TC genesis frequency and track density in individual TC basins were obtained from the Regional and Mesoscale Meteorology Branch (RAMMB) of the National Oceanic and Atmospheric Administration (NOAA)/National Environmental Satellite, Data, and Information Service (NESDIS). TCs in this study were defined as those in the datasets whose maximum wind speeds exceed the minimum threshold of tropical storm intensity (17.2 m s^{-1} or 34 knots). Monthly SST from the Extended Reconstructed sea surface temperature (ERSST) version 4 (Huang et al., 2015) and atmospheric data from the National Centers for Environmental Prediction (NCEP)-National Center for Atmospheric Research (NCAR) reanalysis (Kalnay et al., 1996) were used to explain TC activity from the perspective of large-scale conditions. Monthly precipitation data from the Global Precipitation Climatology Project (Version 2.3, GPCP) (Adler et al., 2018) were used to illustrate the anomalous heating source.

The North Atlantic Oscillation (NAO) index from the NOAA Climate Prediction Center was used to interpret the anomalous TCG in the NA. Following the current 30-year baseline used by NOAA, climatology in this study was defined as the mean state over 1981-2010.

The genesis potential index (GPI), which was developed by Emanuel and Nolan (2004) and modified by Murakami and Wang (2010), was used to examine the impacts of large-scale conditions on TCG. The formula of GPI is as follows:

$$\mathrm{GPI} = |10^5\eta|^{\frac{3}{2}}\left(\frac{\mathcal{H}}{50}\right)^3\left(\frac{Vp}{70}\right)^3(1+0.1Vshear)^{-2}\left(\frac{-\omega+0.1}{0.1}\right)$$

where η is the absolute vorticity (s^{-1}) at 850 hPa, $\mathcal{H}$ is the relative humidity (%) at 600 hPa, Vp is the maximum potential intensity (Bister & Emanuel, 1998; K. A. Emanuel, 1995) in m s^{-1}, $Vshear$ is the magnitude of the vertical wind shear (m s^{-1}) between 850 and 200 hPa, and ω is the 500-hPa vertical pressure velocity (Pa s^{-1}).

To illustrate the impacts of subtropical NP SST on the large-scale circulation during the 2018 TC season, two numerical experiments were conducted with a coupled climate system model (Cao et al., 2015). One is a control run with external forcings (solar, volcanic, and greenhouse gases) fixed at 1990 conditions. The other is a sensitivity run in which the conditions were the same as those in the control run except for subtropical NP SST warming, which was nudged in the coupled climate model toward the 2018 observation(see B. Wang et al., 2018 for details). Each experiment included a 60-yr integration, with the last 30 years used to construct the ensemble mean. The difference between the two experiments was regarded as the atmospheric response to the NP SST anomalies.

3. Unprecedented Northern Hemisphere TC activity in June-September of 2018

The extremely active TCG in 2018 mainly occurred in June-July-August-September (JJAS) (Fig. 2a). Therefore, we focused on JJAS to highlight these anomalous months. The results when June-October or June-November were considered were similar to those for June-September. 53 TCs were observed in JJAS 2018, which was 15 or 40% more than the climatology. This is the highest on record since 1965 (Fig. 2b). Figure 2c shows TCG in the NIO, the WNP, the ENP and the NA. Note that enhanced NA TCG predominantly occurred in the subtropical NA (north of 30° N, Fig. 2c). The anomalous TCG in the NA only accounted for about 20% of the total NH TCG anomalies, while the rest was contributed by the NP (Fig. 2c). Forty-one TCs occurred in JJAS 2018 in the NP, which was 1.4 times its climatological average.

Figure 3a and b show the spatial distributions of anomalous TCG and track density during JJAS 2018. In the WNP, enhanced TC formation mainly occurred along a southeast-northwest oriented zone extending from the eastern Philippine Sea to the vicinity of Taiwan, while in the ENP, positive TCG anomalies were observed to the east of 130° W. Over the NA, increased TCG was observed in the tropical eastern Atlantic and in the subtropics. Notably, in 2018 more TCs took a northward-recurving track in the WNP, thereby influencing eastern China, the Korean Peninsula and Japan. In the ENP, due to increased genesis frequency and westward-steering flow, more TCs moved westward to the CNP and thus impacted the Hawaiian Islands (Fig. 3b). Here we used named storm days to quantify these salient features of TC tracks in 2018 (B. Wang et al., 2010). Due to a remarkable increase in the number of

northward-recurving tracks in the WNP, the number of named storm days in the subtropical WNP (25° N-40° N, 120° E-145° E) was the highest since 1965 (Fig. 3c). Such a track change can be attributed to enhanced TCG in a southeast-northwest oriented zone (Fig. 3a) and anomalous cyclonic steering flow over the subtropical WNP (Fig. 3b). The latter can prevent TCs from entering tropical southeast Asia and steering them towards subtropical East Asia (C. Wang & Wu, 2015; L. Wu et al., 2005). Meanwhile, enhanced TC formation in the ENP induced more TCs to move westward following the climatological trade winds. Thus the eastern-central tropical NP experienced increased named storm days in JJAS 2018 (Fig. 3c).

4. Interpretation

To see how the large-scale circulation and related environmental parameters affected the unprecedented NH TC activity in JJAS 2018, we first examined the spatial patterns of the anomalous GPI and the contributions of individual environmental parameters. Figure 4a shows that the distribution of the total GPI anomalies can well reproduce observed TCG anomalies over the WNP, while it only marginally reproduced observed TCG anomalies over the ENP and the central subtropical NA. A large mismatch can be seen in the central-eastern North Pacific trade wind region.

North Pacific

What caused these changes in favorable large-scale conditions? We find that these changes over the NP were tightly linked to a weakened NP subtropical high (NPSH) (Fig. 5a),

which provided an anomalous cyclonic circulation and anomalous ascending motion in the entire NP and thus favored TCG in both the WNP and the ENP. How can this weakened NPSH persist through JJAS? We propose that a positive atmosphere-ocean thermodynamic feedback between the anomalous cyclonic circulation and underlying SST anomalies may play a critical role. The anomalous cyclonic circulation was accompanied by positive SST anomalies in a southwest-northeast oriented zone stretching from the tropical central Pacific to the subtropical west coast of North America. The sea surface warming in this region enhanced local precipitation so that precipitation anomalies tended to coincide with warm SST anomalies. Both precipitation anomalies and warm SST anomalies were located to the east and south of the anomalous NP cyclonic circulation (Fig. 5a). This coupled pattern suggests a positive feedback between the NP anomalous cyclone and the elongated warming and enhanced convection in the tropics (Chiang & Vimont, 2004; B. Wang et al., 2000, 2003). More specifically, the southwest-northeast oriented anomalous atmospheric heating (as indicated by precipitation anomalies) can stimulate an anomalous cyclonic circulation to its west and north as a Rossby wave response. The surface westerly and southwesterly anomalies to the eastern flank of the anomalous cyclonic circulation can, in turn, warm the underlying ocean surface. This is because west southwesterly winds superimpose on the mean northeasterly trades, thereby reducing the total wind speed and weakening sea surface evaporation and entrainment cooling (B. Wang et al., 2000, 2003). Such an atmosphere-ocean feedback mechanism for maintaining the subtropical high has been confirmed by numerical experiments with coupled atmosphere-ocean models (N.-C. Lau et al., 2004; N. C. Lau & Nath, 2003; B. Wang et al.,

2013; Xiang et al., 2013). It was this positive air-sea feedback that maintained both the weakened NPSH and the associated SST warming. Such a weakening of the NPSH created positive low-level vorticity and mid-level ascending motion in the NP; the latter can further transport low-level moisture to the middle troposphere, increasing lower tropospheric relative humidity and favoring TCG over the WNP (Murakami & Wang, 2010). Besides these favorable environmental conditions, SST warming tended to increase the maximum potential intensity over the ENP (K. A. Emanuel, 1987), providing a conducive thermodynamic environment for TC formation as well (K. A. Emanuel & Nolan, 2004). As a result, the maximum potential intensity term was a significant contributor to the positive GPI anomalies in the ENP (Fig. 4d). In order to test the proposed role of the subtropical NP SST anomalies in NP TCG, numerical experiments were conducted by using a coupled climate model (see section 2). With the subtropical NP SST warming in JJAS 2018 nudged to the coupled model, it reproduced the observed cyclonic circulation anomaly over the NP (i.e., weakened NPSH, Fig. 4d). Accordingly, the corresponding large-scale conditions (represented by the GPI) were consistent with the observed active NP TCG (figure not shown). However, the wind responses to SST warming were relatively weak compared to the observation in the tropical eastern NP and the subtropical NP. These discrepancies may result from the un-nudged SST anomalies in the NA and the subtropical NP. For example, the SST cooling in the tropical North Atlantic can induce a Walker Circulation-type response in the eastern NP, which may amplify the simulated wind responses to the SST warming in the tropical NP(Caron et al., 2015; Patricola et al., 2017; Smith et al., 2010; Wood et al., 2019). Generally, numerical results further confirmed the

proposed crucial role of subtropical NP SST warming in the anomalous NP TCG during the 2018 TC season.

Do the proposed role of the NPSH and the related maintaining mechanism remain valid for active NP TCG in other years? To answer this question, we further examined the historical records. Based on the best track data since 1965, we selected seven high-frequency TCG years (1967, 1982, 1985, 1989, 1992, 1994 and 2016) and seven low-frequency TCG years (1969, 1977, 1979, 1998, 1999, 2007 and 2010) to make a composite analysis of the corresponding anomalous large-scale circulation. The composite difference between the high and low-frequency years featured a weakened NPSH and sea surface warming in an elongated southwest-northeast oriented zone over the tropical NP (Fig. 5a), which can be found in the results derived from JJAS 2018 (Figs. 4c and 5a). The weakened NPSH can favor WNP TCG through increasing positive low-level vorticity and mid-level ascending motion (Gray, 1968; C. Wang & Wang, 2019). For the ENP, the subtropical NP SST warming enhances maximum potential intensity (Emanuel, 1987), ascending motion and mid-level humidity, thus favoring ENP TCG. To confirm the close connection between subtropical NP SST, NPSH and NP TCG, their temporal evolutions during 1965-2018 were examined (Fig. 5a). A meridional shear index was defined by the anomalous zonal winds at 850 hPa to measure the strength of the NPSH: NPSH index = U850 (30° N-40° N, 110° E-150° W) – U850 (5° N-15° N, 110° E-150° W). The two regions generally coincide with the climatological subtropical westerly and tropical easterly winds associated with the NPSH, respectively (Fig. 5a). Positive values of the meridional shear index represent an enhanced NPSH. Note that the tropical mean SST was

removed from the time series of the subtropical NP SST (Johnson & Xie, 2010; Knutson et al., 2008; Vecchi & Soden, 2007). Indeed, temporal evolutions of subtropical NP SST, NPSH and NP TCG were significantly correlated with each other ($|r|>0.57$, $P<0.01$), indicating the considerable impact that subtropical NP SST exerts on TC genesis through modification of the NPSH. In fact, the temporal evolution of subtropical NP SST was significantly correlated with that of the Pacific Meridional Mode (PMM, Chiang & Vimont, 2004) index with a correlation coefficient of 0.78 over 1965-2018. This close connection suggested their similar effects on TC activity in the WNP (C. Wang, Wu, et al., 2019; Y.-K. Wu et al., 2018; Zhan et al., 2017; W Zhang et al., 2016) and the ENP (Collins et al., 2016; Murakami et al., 2017; Wood et al., 2019). Because the PMM index is operationally monitored (http://www.aos.wisc.edu/~dvimont/MModes/PMM.html), these results have important implications for improving the prediction skill of TC activity in the NH.

However, SST warming in 2018 was not extreme (Fig. 5b), so why was the 2018 TC season so active? Previous studies have suggested that both the SST-induced pressure gradient and the convective heating anomalies play important roles in large-scale circulation changes (Gill, 1980; Lindzen and Nigam, 1987). Therefore, we further explored the convective heating anomaly (represented by the precipitation anomaly) over the subtropical NP in JJAS 2018. Figure 5c shows the time series of the GPCP subtropical NP precipitation anomalies over 1979-2018. The precipitation anomaly in 2018 was the second-highest on record, which is in accordance with the extremely high NP TC genesis frequency in 2018. Moreover, the greatest JJAS precipitation value measured in 1994 also matched the highest TC genesis frequency in

the NP. Precipitation and TCG are significantly correlated with a correlation coefficient of 0.63 ($P<0.01$). These results suggest that there is an essential role of subtropical NP SST warming and related convective heating in the occurrence of extreme NP TCG during JJAS 2018. Additionally, SST cooling in the tropical NA can induce a Walker Circulation-type response across the NP, influencing TC activity in the NP (Caron et al., 2015; Ham et al., 2013; Huo et al., 2015; Patricola et al., 2017; Smith et al., 2010; C. Wang & Wang, 2019; Wood et al., 2019; W Zhang et al., 2016). However, the magnitude of the SST cooling in the tropical NA was much weaker than that of SST warming in the subtropical NP in JJAS 2018 (Fig. 4c). Therefore, the tropical NA SST cooling may play a secondary role in the extreme TCG in the NP in JJAS 2018.

North Atlantic

Although the NP produced most of the anomalous NH TC activity in JJAS 2018, active TCG in the NP does not guarantee extreme TCG frequency in the NH. For example, the NP experienced the greatest TCG frequency in 1994 (Fig. 5c), but the total TCG frequency in the NH for that year ranked second among those after 1965 (Fig. 2b). This is due to the extremely low TCG in the NA in 1994, which was the final season of the most recent Atlantic low-activity era (Avila & Rappaport, 1996; Goldenberg et al., 2001). However, Atlantic hurricane activity has been well above average since 1995, which can be attributed to global warming (J B Elsner et al., 2008; K. Emanuel, 2005; Holland & Webster, 2007), the Atlantic Multidecadal Oscillation (AMO) (Goldenberg et al., 2001) and the Atlantic Meridional Mode (AMM)

(Kossin & Vimont, 2007; Vimont & Kossin, 2007). It was the above-average TCG frequency in the NA and the extreme genesis frequency in the NP that jointly contributed to the unprecedented 2018 TC season. Interestingly, the TCG frequency in the tropical NA (south of 30° N) during June-September of 2018 was close to its climatological average over 1981-2010 (figure not shown). The enhanced NA TCG in JJAS 2018 occurred mainly in the subtropics (north of 30° N, Fig. 3a). It was found that enhanced TCG in the subtropical NA was closely linked to the positive phase of NAO, which features the canonical tri-pole SST pattern (Hurrell, 1995; Visbeck et al., 2001, Fig. 5a). The associated subtropical SST warming can enhance TCG by increasing maximum potential intensity (Fig. 4). Moreover, the subtropical NA SST warming can strengthen ascending motion and thus further increase cyclonic vorticity in the western/central subtropical NA. These dynamic parameters play a secondary role in enhancing TC formation over the subtropical NA. Considering that the NAO index in JJAS 2018 was at its most positive value since 1965 (figure not shown), we argue that the extremely positive phase of NAO is a plausible cause for the active subtropical NA TCG in 2018. It should be noted that four of the five TCs that formed north of 30° N were originally subtropical cyclones (i.e., Debby, Ernesto, Joyce and Leslie). The result is consistent with previous studies that discussed the relationship of the NAO with TCs in the subtropical NA (Boudreault et al., 2017; James B Elsner & Kara, 1999; Kossin et al., 2010; Kozar et al., 2012). Because most NA TCs form in August-October, we examined the results when only August-September of 2018 were considered, which were generally similar to those for JJAS 2018.

4. Conclusion and discussion

The 2018 NH TC season is indeed an exceptional season, as TCG frequency during June-September of this year is the greatest since 1965. The unusual TCG frequency results from enhanced TCG in the NP and in the subtropical NA. For the NP basin, active TCG can be attributed to favorable large-scale conditions that are tightly linked to the persistent weakening of the NPSH and subtropical NP SST warming. Such a linkage was further confirmed by numerical experiments and comparisons with historical records. The JJAS NPSH intensity index, the NP TCG frequency, and the subtropical NP SST warming are significantly correlated with each other ($|r|>0.57$, $P<0.01$) over the past 54 years (1965–2018). Over the NA, above-normal TCG occurred in the subtropics, which is tightly linked to subtropical SST warming associated with the positive phase of NAO. The subtropical NA SST warming can enhance TCG by providing favorable large-scale thermodynamic and dynamic environments. The result here has important implications for seasonal forecasting of TC activity in the NP and for understanding TC activity on the hemisphere-scale.

Variations in the NPSH have been known to be closely related to the underlying subtropical NP SST (Chiang & Vimont, 2004; B. Wang et al., 2000, 2003; Zhao et al., 2019). Interestingly, the previous negative SST anomaly in the subtropical NP became positive since 2013. Such a transition occurred around the same time as the termination of the global warming hiatus and the phase change in the Pacific Decadal Oscillation (Fyfe et al., 2016; Meehl et al., 2016). Additionally, some recent studies found that anomalous subtropical NP warming was responsible for the failure in seasonal forecasting of the 2016 WNP TC season following the

2015-2016 El Niño event(Chen & Wang, 2018; C. Wang, Wu, et al., 2019; Y.-K. Wu et al., 2018; Yamada et al., 2019; Zhan et al., 2017). Specifically, the WNP usually experiences an inactive TC season following a strong El Niño event due to the existence of an anomalous anti-cyclonic circulation, which is coupled to the underlying SST cooling in the NP (B. Wang et al., 2000; B. Wang & Chan, 2002). However, SST warming occurred in the subtropical NP during the TC peak season following the strong 2015-2016 El Niño event. The subtropical NP SST warming stimulated an anomalous cyclonic circulation, induced a convergence zone over the WNP and thus led to active TC activity during the 2016 TC peak season (C. Wang, Wu, et al., 2019; Y.-K. Wu et al., 2018; Zhan et al., 2017). These facts suggest that subtropical NP SST warming may play a vital role in climate variability. Therefore, the roles of internal variability and external forcing in the evolution of subtropical NP SST deserve future exploration. We note that there are some discrepancies among the intensity records from different operational centers in the WNP and the NIO. Therefore, we only discussed TCG frequency and track in the 2018 TC season. The intensity of 2018 TCs also deserves further exploration.

Acknowledgement:

The authors thank Dr. Suzana Camargo, Dr. Phil Klotzbach and an anonymous reviewer for their important suggestions for improving the manuscript. This study was jointly supported by the National Natural Science Foundation of China (Grant No. 41705060, 41420104002, 41730961, 41675072 and 41605032), the Natural Science Foundation of Jiangsu Province (BK20170941 and BK20171095) and the National Key Research and Development Program

of China (Grant No. 2016YFA0600401). This is the School of Ocean and Earth Science and Technology (SOEST) publication number XXXX, the ESMC publication number XXX, and the IPRC publication number YYYY. The NCEP reanalysis data are available at https://www.esrl.noaa.gov/psd/data/reanalysis/reanalysis.shtml. The best track data from the JTWC are available at http://www.usno.navy.mil/NOOC/ nmfcph/RSS/jtwc/best_tracks. The NHC best track data are available at https://www.nhc.noaa.gov/data/. The 2018 best track data are available at http://rammb.cira.colostate.edu/products/tc_realtime/season.asp?storm_season=2018. The NOAA SST data set is available at https://www. esrl. noaa.gov/psd/data/gridded/data. noaa.ersst.v4.html. The GPCP precipitation data are available at https://www.esrl.noaa.gov/psd/data/gridded/data.gpcp.html. The NAO index is available at https://www.cpc.ncep.noaa.gov/products/precip/CWlink/pna/nao.shtml. The Oceanic Nino Index is available at https://origin.cpc.ncep.noaa.gov/products/analysis_monitoring/ensostuff/ONI_v5.php.

References:

Adler, R. F., Sapiano, M. R. P., Huffman, G. J., Wang, J. J., Gu, G., Bolvin, D., et al. (2018). The Global Precipitation Climatology Project (GPCP) monthly analysis (New Version 2.3) and a review of 2017 global precipitation. *Atmosphere*, *9*(4), 138. https://doi.org/10.3390/atmos9040138

Avila, L. A., & Rappaport, E. N. (1996). Atlantic Hurricane Season of 1994. *Monthly Weather Review*, *124*(7), 1558–1578. https://doi.org/10.1175/1520-0493(1996)124<1558:AHSO>2.0.CO;2

Bister, M., & Emanuel, K. A. (1998). Dissipative heating and hurricane intensity. *Meteorology and Atmospheric Physics*, *65*(3–4), 233–240.

Boudreault, M., Caron, L.-P., & Camargo, S. J. (2017). Reanalysis of climate influences on Atlantic tropical cyclone activity using cluster analysis. *Journal of Geophysical Research: Atmospheres*, *122*(8), 4258–4280. https://doi.org/10.1002/2016JD026103

Camargo, S. J., & Sobel, A. H. (2005). Western North Pacific tropical cyclone intensity and ENSO. *Journal of Climate*, *18*(15), 2996–3006. https://doi.org/10.1175/JCLI3457.1

Camargo, S. J., Robertson, A. W., Barnston, A. G., & Ghil, M. (2008). Clustering of eastern North Pacific tropical cyclone tracks: ENSO and MJO effects. *Geochemistry, Geophysics, Geosystems*, *9*(6), n/a-n/a. https://doi.org/10.1029/2007gc001861

Camargo, S. J., Sobel, A. H., Barnston, A. G., & Klotzbach, P. J. (2010). The Influence of Natural Climate Variability on Tropical Cyclones, and Seasonal Forecasts of Tropical Cyclone Activity. In C. Johnny C L & K. Jeffrey D (Eds.), *Global Perspectives on Tropical Cyclones* (pp. 325–360). World Scientific. https://doi.org/10.1142/9789814293488_0011

Cao, J., Wang, B., Xiang, B., Li, J., Wu, T., Fu, X., et al. (2015). Major modes of short-term climate variability in the newly developed NUIST Earth System Model (NESM). *Advances in Atmospheric Sciences*. https://doi.org/10.1007/s00376-014-4200-6

Caron, L. P., Boudreault, M., & Camargo, S. J. (2015). On the variability and predictability of eastern pacific tropical cyclone activity. *Journal of Climate*, *28*(24), 9678–9696. https://doi.org/10.1175/JCLI-D-15-0377.1

Chan, J. C. L. (1985). Tropical cyclone activity in the northwest Pacific in relation to the El Niño/Southern Oscillation phenomenon. *Monthly Weather Review*, *113*(4), 599–606.

Chen, G., & Wang, K. (2018). Why is the tropical cyclone activity over the western north pacific so distinct in 2016 and 1998 following super El niño events? *Journal of the Meteorological Society of Japan*, *96*(2), 97–110. https://doi.org/10.2151/jmsj.2018-013

Chiang, J. C. H., & Vimont, D. J. (2004). Analogous Pacific and Atlantic Meridional Modes of Tropical Atmosphere – Ocean Variability. *Journal of Climate*, *17*(21), 4143–4158. https://doi.org/10.1175/JCLI4953.1

Chu, J.-H., Sampson, C. R., Levine, A. S., & Fukada, E. (2002). *The joint typhoon warning center tropical cyclone best-tracks, 1945–2000*. *Ref. NRL/MR/7540-02-16*. Washington, D. C: Nav. Res. Lab. https://doi.org/www.usno.navy.mil/NOOC/nmfc-ph/RSS/jtwc/best_tracks/TC_bt_report.html

Chu, P S. (2004). ENSO and tropical cyclone activity. Hurricanes and Typhoons: Past,

Present, and Potential, RJ Murnane and K.-B. Liu, Eds. *Columbia University Press*, *297*, 332.

Chu, Pao Shin, & Clark, J. D. (1999). Decadal Variations of Tropical Cyclone Activity over the Central North Pacific. *Bulletin of the American Meteorological Society*, *80*(9), 1875–1881. https://doi.org/10.1175/1520-0477(1999)080<1875:DVOTCA>2.0.CO;2

Clark, J. D., & Chu, P.-S. (2002). Interannual Variation of Tropical Cyclone Activity over the Central North Pacific. *Journal of the Meteorological Society of Japan*, *80*(3), 403–418. https://doi.org/10.2151/jmsj.80.403

Collins, J. M., Klotzbach, P. J., Maue, R. N., Roache, D. R., Blake, E. S., Paxton, C. H., & Mehta, C. A. (2016). The record-breaking 2015 hurricane season in the eastern North Pacific: An analysis of environmental conditions. *Geophysical Research Letters*, *43*(17), 9217–9224. https://doi.org/10.1002/2016GL070597

Elsner, J B, Kossin, J. P., & Jagger, T. H. (2008). The increasing intensity of the strongest tropical cyclones. *Nature*, *455*(7209), 92–95. https://doi.org/10.1038/nature07234

Elsner, James B, & Kara, A. B. (1999). *Hurricanes of the North Atlantic: Climate and society*. New York: Oxford University Press.

Emanuel, K. (2005). Increasing destructiveness of tropical cyclones over the past 30 years. *Nature*, *436*(7051), 686–688. https://doi.org/10.1038/nature03906

Emanuel, K. A. (1987). The dependence of hurricane intensity on climate. *Nature*, *326*(6112), 483–485.

Emanuel, K. A. (1995). Sensitivity of tropical cyclones to surface exchange coefficients and a revised steady-state model incorporating eye dynamics. *Journal of the Atmospheric Sciences*, *52*(22), 3969–3976.

Emanuel, K. A., & Nolan, D. S. (2004). Tropical cyclone activity and the global climate system. In *Preprints, 26th Conf. on Hurricanes and Tropical Meteorology, Miami, FL, Amer. Meteor. Soc. A* (Vol. 10).

Frank, W. M., & Young, G. S. (2007). The Interannual Variability of Tropical Cyclones. *Monthly Weather Review*, *135*(10), 3587–3598. https://doi.org/10.1175/mwr3435.1

Fyfe, J. C., Meehl, G. A., England, M. H., Mann, M. E., Santer, B. D., Flato, G. M., et al. (2016). Making sense of the early-2000s warming slowdown. *Nature Climate Change*, *6*(3), 224–228. https://doi.org/10.1038/nclimate2938

Goldenberg, S. B., & Shapiro, L. J. (1996). Physical mechanisms for the association of El Niño and west African rainfall with Atlantic major hurricane activity. *Journal of Climate*, *9*(6), 1169–1187. https://doi.org/10.1175/1520-0442(1996)009<1169:PMFTAO>2.0.CO;2

Goldenberg, S. B., Landsea, C. W., Mestas-Nuñez, A. M., Gray, W. M., Mestas-Nunez, A. M., & Gray, W. M. (2001). The recent increase in Atlantic hurricane activity: Causes and implications. *Science*, *293*(5529), 474–479. https://doi.org/10.1126/science.1060040

Gray, W. M. (1968). Global view of the origin of tropical disturbances and storms. *Monthly Weather Review*, *96*(10), 669–700.

Gray, W. M. (1984). Atlantic seasonal hurricane frequency. Part I: El Nino and 30 mb quasi-biennial oscillation influences. *Monthly Weather Review*, *112*(9), 1649–1668.

Ham, Y.-G., Kug, J.-S., Park, J.-Y., & Jin, F.-F. (2013). Sea surface temperature in the north tropical Atlantic as a trigger for El Niño/Southern Oscillation events. *Nature Geoscience*, *6*(2), 112–116. https://doi.org/10.1038/ngeo1686

Holland, G. J., & Webster, P. J. (2007). Heightened tropical cyclone activity in the North Atlantic: natural variability or climate trend? *Philos Trans A Math Phys Eng Sci*, *365*(1860), 2695–2716. https://doi.org/10.1098/rsta.2007.2083

Huang, B., Banzon, V. F., Freeman, E., Lawrimore, J., Liu, W., Peterson, T. C., et al. (2015). Extended reconstructed sea surface temperature version 4 (ERSST.v4). Part I: Upgrades and intercomparisons. *Journal of Climate*, *28*(3), 911–930. https://doi.org/10.1175/JCLI-D-14-00006.1

Huo, L., Guo, P., Hameed, S. N., & Jin, D. (2015). The role of tropical Atlantic SST anomalies in modulating western North Pacific tropical cyclone genesis. *Geophysical Research Letters*, *42*(7), 2378–2384. https://doi.org/10.1002/2015GL063184

Hurrell, J. W. (1995). Decadal Trends in the North Atlantic Oscillation: Regional Temperatures and Precipitation. *Science*, *269*(5224), 676–679. https://doi.org/10.1126/science.269.5224.676

India Meteorological Department (2008) Tracks of cyclones and depressions (1891–2007), electronic version 1.0/2008. India Meteorological Department, Chennai

Johnson, N. C., & Xie, S.-P. (2010). Changes in the sea surface temperature threshold for tropical convection. *Nature Geoscience*, *3*(12), 842–845. https://doi.org/10.1038/ngeo1008

Kalnay, E., Kanamitsu, M., Kistler, R., Collins, W., Deaven, D., Gandin, L., et al. (1996). The NCEP/NCAR 40-year reanalysis project. *Bulletin of the American Meteorological Society*, *77*(3), 437–471.

Knutson, T. R., Sirutis, J. J., Garner, S. T., Vecchi, G. A., & Held, I. M. (2008). Simulated reduction in Atlantic hurricane frequency under twenty-first-century warming conditions. *Nature Geoscience*, *1*(6), 359–364. https://doi.org/10.1038/ngeo202

Kossin, J. P., & Vimont, D. J. (2007). A more general framework for understanding atlantic hurricane variability and trends. *Bulletin of the American Meteorological Society*, *88*(11), 1767–1781. https://doi.org/10.1175/BAMS-88-11-1767

Kossin, J. P., Camargo, S. J., & Sitkowski, M. (2010). Climate Modulation of North Atlantic Hurricane Tracks. *Journal of Climate*, *23*(11), 3057–3076. https://doi.org/10.1175/2010JCLI3497.1

Kozar, M. E., Mann, M. E., Camargo, S. J., Kossin, J. P., & Evans, J. L. (2012). Stratified statistical models of North Atlantic basin-wide and regional tropical cyclone counts. *Journal of Geophysical Research: Atmospheres*, *117*(D18), n/a-n/a. https://doi.org/10.1029/2011JD017170

Lander, M. A. (1994). An Exploratory Analysis of the Relationship between Tropical Storm Formation in the Western North Pacific and ENSO. *Monthly Weather Review*, *122*(4), 636–651. https://doi.org/10.1175/1520-0493(1994)122<0636:AEAOTR>2.0.CO;2

Landsea, C. W., & Franklin, J. L. (2013). Atlantic Hurricane Database Uncertainty and Presentation of a New Database Format. *Monthly Weather Review*, *141*(10), 3576–3592.

https://doi.org/10.1175/MWR-D-12-00254.1

Lau, N.-C., Nath, M. J., & Wang, H. (2004). Simulations by a GFDL-GCM of ENSO related variability of the coupled atmosphere-ocean system in the East Asia monsoon region. In C.-P. Chang (Ed.), *East Asian Monsoon* (pp. 271–300). World Scientific. https://doi.org/10.1142/9789812701411_0007

Lau, N. C., & Nath, M. J. (2003). Atmosphere-ocean variations in the Indo-Pacific sector during ENSO episodes. *Journal of Climate*, *16*(1), 3–20. https://doi.org/10.1175/1520-0442(2003)016<0003:AOVITI>2.0.CO;2

Maue, R. N. (2009). Northern Hemisphere tropical cyclone activity. *Geophysical Research Letters*, *36*(5), L05805. https://doi.org/10.1029/2008GL035946

Meehl, G. A., Hu, A., & Teng, H. (2016). Initialized decadal prediction for transition to positive phase of the Interdecadal Pacific Oscillation. *Nature Communications*, *7*. https://doi.org/10.1038/ncomms11718

Murakami, H., & Wang, B. (2010). Future change of North Atlantic tropical cyclone tracks: Projection by a 20-km-mesh global atmospheric model. *Journal of Climate*, *23*(10), 2699–2721. https://doi.org/10.1175/2010JCLI3338.1

Murakami, H., Vecchi, G. A., Delworth, T. L., Wittenberg, A. T., Underwood, S., Gudgel, R., et al. (2017). Dominant Role of Subtropical Pacific Warming in Extreme Eastern Pacific Hurricane Seasons: 2015 and the Future. *Journal of Climate*, *30*(1), 243–264. https://doi.org/10.1175/JCLI-D-16-0424.1

Patricola, C. M., Saravanan, R., & Chang, P. (2014). The Impact of the El Niño–Southern Oscillation and Atlantic Meridional Mode on Seasonal Atlantic Tropical Cyclone Activity. *Journal of Climate*, *27*(14), 5311–5328. https://doi.org/10.1175/jcli-d-13-00687.1

Patricola, C. M., Saravanan, R., & Chang, P. (2017). A teleconnection between Atlantic sea surface temperature and eastern and central North Pacific tropical cyclones. *Geophysical Research Letters*, *44*(2), 1167–1174. https://doi.org/10.1002/2016GL071965

Singh, O. P., Ali Khan, T. M., & Rahman, M. S. (2000). Changes in the frequency of tropical cyclones over the North Indian Ocean. *Meteorology and Atmospheric Physics*, *75*(1–2), 11–20. https://doi.org/10.1007/s007030070011

Smith, D. M., Eade, R., Dunstone, N. J., Fereday, D., Murphy, J. M., Pohlmann, H., & Scaife, A. A. (2010). Skilful multi-year predictions of Atlantic hurricane a frequency. *Nature Geoscience*, *3*(12), 846–849. https://doi.org/10.1038/ngeo1004

Sobel, A. H., Camargo, S. J., Barnston, A. G., & Tippett, M. K. (2016). Northern hemisphere tropical cyclones during the quasi-El Niño of late 2014. *Natural Hazards*. https://doi.org/10.1007/s11069-016-2389-7

Tang, B. H., & Neelin, J. D. (2004). ENSO Influence on Atlantic hurricanes via tropospheric warming. *Geophysical Research Letters*, *31*(24), 1–4. https://doi.org/10.1029/2004GL021072

Vecchi, G. A., & Soden, B. J. (2007). Effect of remote sea surface temperature change on tropical cyclone potential intensity. *Nature*, *450*(7172), 1066–1070. https://doi.org/10.1038/nature06423

Vimont, D. J., & Kossin, J. P. (2007). The Atlantic Meridional Mode and hurricane activity. *Geophysical Research Letters*, *34*(7). https://doi.org/10.1029/2007gl029683

Visbeck, M. H., Hurrell, J. W., Polvani, L., & Cullen, H. M. (2001). *The North Atlantic Oscillation: Past, present, and future*. *PNAS November* (Vol. 6).

Wang, B., & Chan, J. C. L. (2002). How strong ENSO events affect tropical storm activity over the western North Pacific. *Journal of Climate*, *15*(13), 1643–1658. https://doi.org/10.1175/1520-0442(2002)015<1643:HSEEAT>2.0.CO;2

Wang, B., Wu, R., & Fu, X. (2000). Pacific–East Asian Teleconnection: How Does ENSO Affect East Asian Climate? *Journal of Climate*, *13*(9), 1517–1536. https://doi.org/10.1175/1520-0442(2000)013<1517:PEATHD>2.0.CO;2

Wang, B., Wu, R., & Li, T. I. M. (2003). Atmosphere-Warm Ocean Interaction and Its Impacts on Asian-Australian Monsoon Variation*. *Journal of Climate*, *16*(8), 1195–1211. https://doi.org/10.1175/1520-0442(2003)16<1195:AOIAII>2.0.CO;2

Wang, B., Yang, Y., Ding, Q.-H., Murakami, H., & Huang, F. (2010). Climate control of the global tropical storm days (1965-2008). *Geophysical Research Letters*, *37*(7), n/a-n/a. https://doi.org/10.1029/2010GL042487

Wang, B., Xiang, B., & Lee, J.-Y. (2013). Subtropical High predictability establishes a promising way for monsoon and tropical storm predictions. *Proceedings of the National Academy of Sciences*, *110*(8), 2718–2722. https://doi.org/10.1073/pnas.1214626110

Wang, B., Li, J., Cane, M. A., Liu, J., Webster, P. J., Xiang, B., et al. (2018). Towards predicting changes in the land monsoon rainfall a decade in advance. *Journal of Climate*, JCLI-D-17-0521.1. https://doi.org/10.1175/JCLI-D-17-0521.1

Wang, C., & Wang, B. (2019). Tropical cyclone predictability shaped by western Pacific subtropical high: integration of trans-basin sea surface temperature effects. *Climate Dynamics*, *53*(5–6), 2697–2714. https://doi.org/10.1007/s00382-019-04651-1

Wang, C., & Wu, L. (2015). Influence of future tropical cyclone track changes on their basin-wide intensity over the western North Pacific: Downscaled CMIP5 projections. *Advances in Atmospheric Sciences*, *32*(5), 613–623. https://doi.org/10.1007/s00376-014-4105-4

Wang, C., & Wu, L. (2016). Interannual Shift of the Tropical Upper-Tropospheric Trough and Its Influence on Tropical Cyclone Formation over the Western North Pacific. *Journal of Climate*, *29*(11), 4203–4211. https://doi.org/10.1175/JCLI-D-15-0653.1

Wang, C., Wang, B., & Wu, L. (2019a). A region-dependent seasonal forecasting framework for tropical cyclone genesis frequency in the western North Pacific. *Journal of Climate*, JCLI-D-19-0006.1. https://doi.org/10.1175/JCLI-D-19-0006.1

Wang, C., Wang, B., & Wu, L. (2019b). Abrupt breakdown of the predictability of early season typhoon frequency at the beginning of the twenty-first century. *Climate Dynamics*, *52*(7–8), 3809–3822. https://doi.org/10.1007/s00382-018-4350-9

Wang, C., Wu, L., Zhao, H., Cao, J., & Tian, W. (2019). Is there a quiescent typhoon season over the western North Pacific following a strong El Niño event? *International Journal of Climatology*, *39*(1), 61–73. https://doi.org/10.1002/joc.5782

Wood, K. M., Klotzbach, P. J., Collins, J. M., & Schreck, C. J. (2019). The Record-Setting

2018 Eastern North Pacific Hurricane Season. *Geophysical Research Letters*, 1–10. https://doi.org/10.1029/2019gl083657

Wu, L., Wang, B., & Geng, S. (2005). Growing typhoon influence on east Asia. *Geophysical Research Letters*, *32*(18), n/a-n/a. https://doi.org/10.1029/2005GL022937

Wu, Y.-K., Hong, C.-C., & Chen, C.-T. (2018). Distinct Effects of the Two Strong El Niño Events in 2015-2016 and 1997-1998 on the Western North Pacific Monsoon and Tropical Cyclone Activity: Role of Subtropical Eastern North Pacific Warm SSTA. *Journal of Geophysical Research: Oceans*, *123*(5), 3603–3618. https://doi.org/10.1002/2018JC013798

Xiang, B., Wang, B., Yu, W., & Xu, S. (2013). How can anomalous western North Pacific Subtropical High intensify in late summer? *Geophysical Research Letters*, *40*(10), 2349–2354. https://doi.org/10.1002/grl.50431

Yamada, Y., Kodama, C., Satoh, M., Nakano, M., Nasuno, T., & Sugi, M. (2019). High-Resolution Ensemble Simulations of Intense Tropical Cyclones and Their Internal Variability During the El Niños of 1997 and 2015. *Geophysical Research Letters*, *46*(13), 7592–7601. https://doi.org/10.1029/2019GL082086

Zhan, R., Wang, Y., & Liu, Q. (2017). Salient Differences in Tropical Cyclone Activity over the Western North Pacific between 1998 and 2016. *Journal of Climate*, *30*(24), 9979–9997. https://doi.org/10.1175/JCLI-D-17-0263.1

Zhang, W, Vecchi, G. A., Murakami, H., Villarini, G., & Jia, L. (2016). The Pacific Meridional Mode and the Occurrence of Tropical Cyclones in the Western North Pacific. *Journal of Climate*, *29*(1), 381–398. https://doi.org/10.1175/JCLI-D-15-0282.1

Zhang, Wei, Leung, Y., & Min, J. (2013). North Pacific Gyre Oscillation and the occurrence of western North Pacific tropical cyclones. *Geophysical Research Letters*, *40*(19), 5205–5211. https://doi.org/10.1002/grl.50955

Zhao, H., & Wang, C. (2019). On the relationship between ENSO and tropical cyclones in the western North Pacific during the boreal summer. *Climate Dynamics*, *52*(1–2), 275–288. https://doi.org/10.1007/s00382-018-4136-0

Zhao, H., Wu, L., Wang, C., & Klotzbach, P. J. (2019). Consistent Late Onset of the Western North Pacific Tropical Cyclone Season Following major El Niño Events. *Journal of the Meteorological Society of Japan. Ser. II*, *97*(3), 673–688. https://doi.org/10.2151/jmsj.2019-039

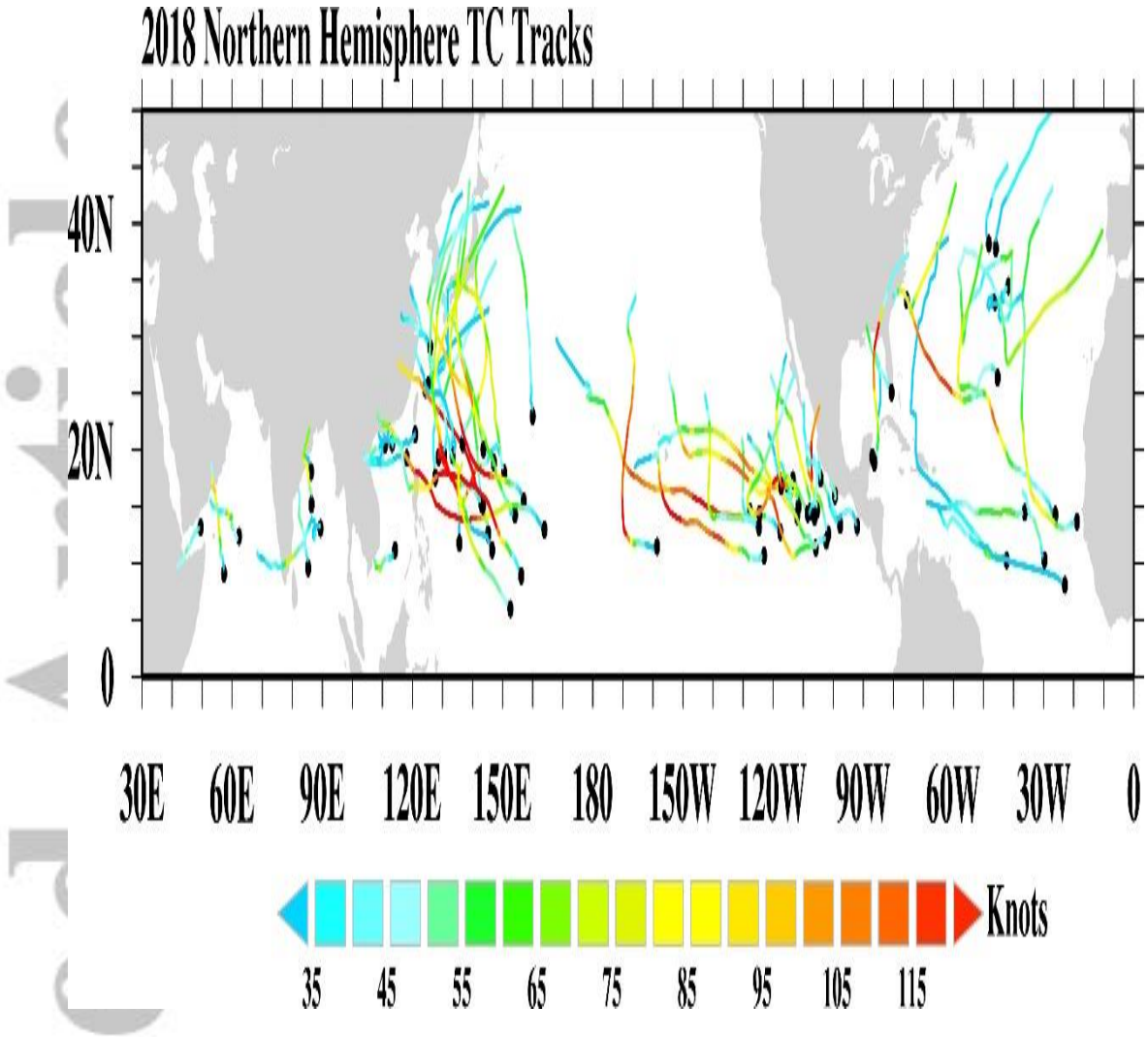

Figure 1. TC tracks and intensities in the Northern Hemisphere (NH) in 2018. The black dots represent TCG locations. The color bar denotes the scale of TC intensity (knots).

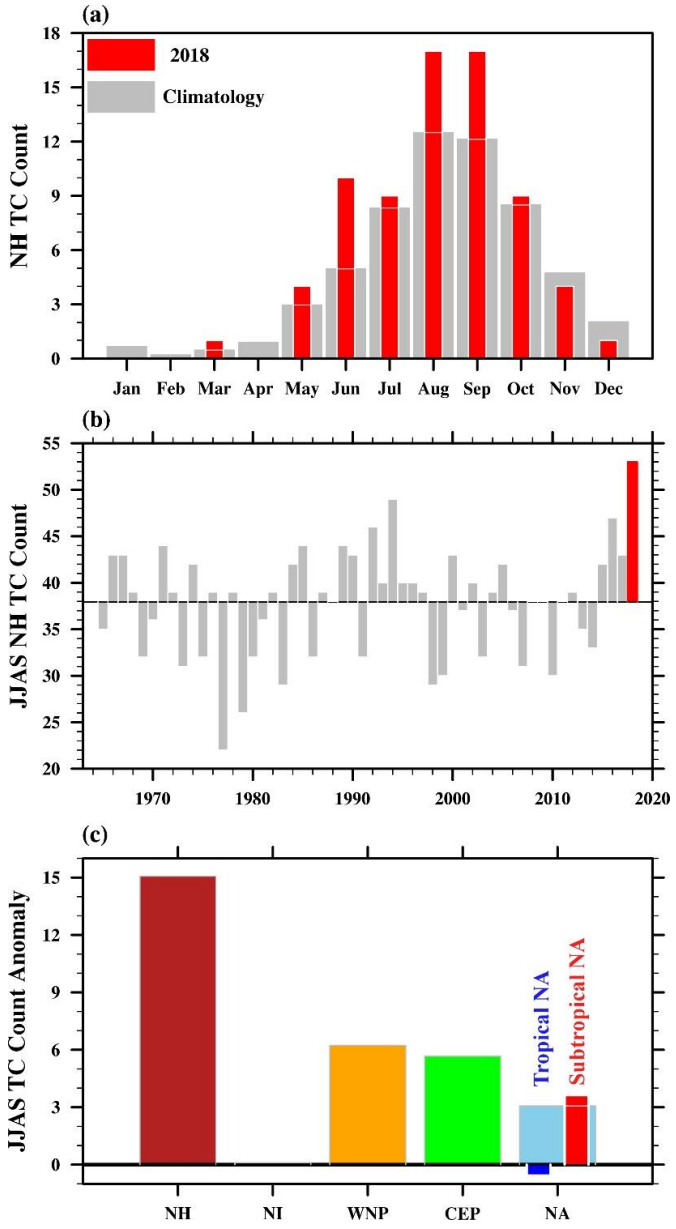

Figure 2. (a) Climatological monthly distribution of NH TCG frequency (grey bars) and in 2018 (red bars), (b) time series of TCG frequency in June-September over the period of 1965-2018, (c) TC count anomalies in the NH and for individual TC basins (North Indian (NI), western North Pacific (WNP), central-eastern North Pacific (CENP) and North Atlantic (NA)) in 2018, with the rightmost blue and red bar representing TC count anomalies in the tropical and subtropical North Atlantic, respectively. The red bar in (b) highlights the greatest TC count in 2018.

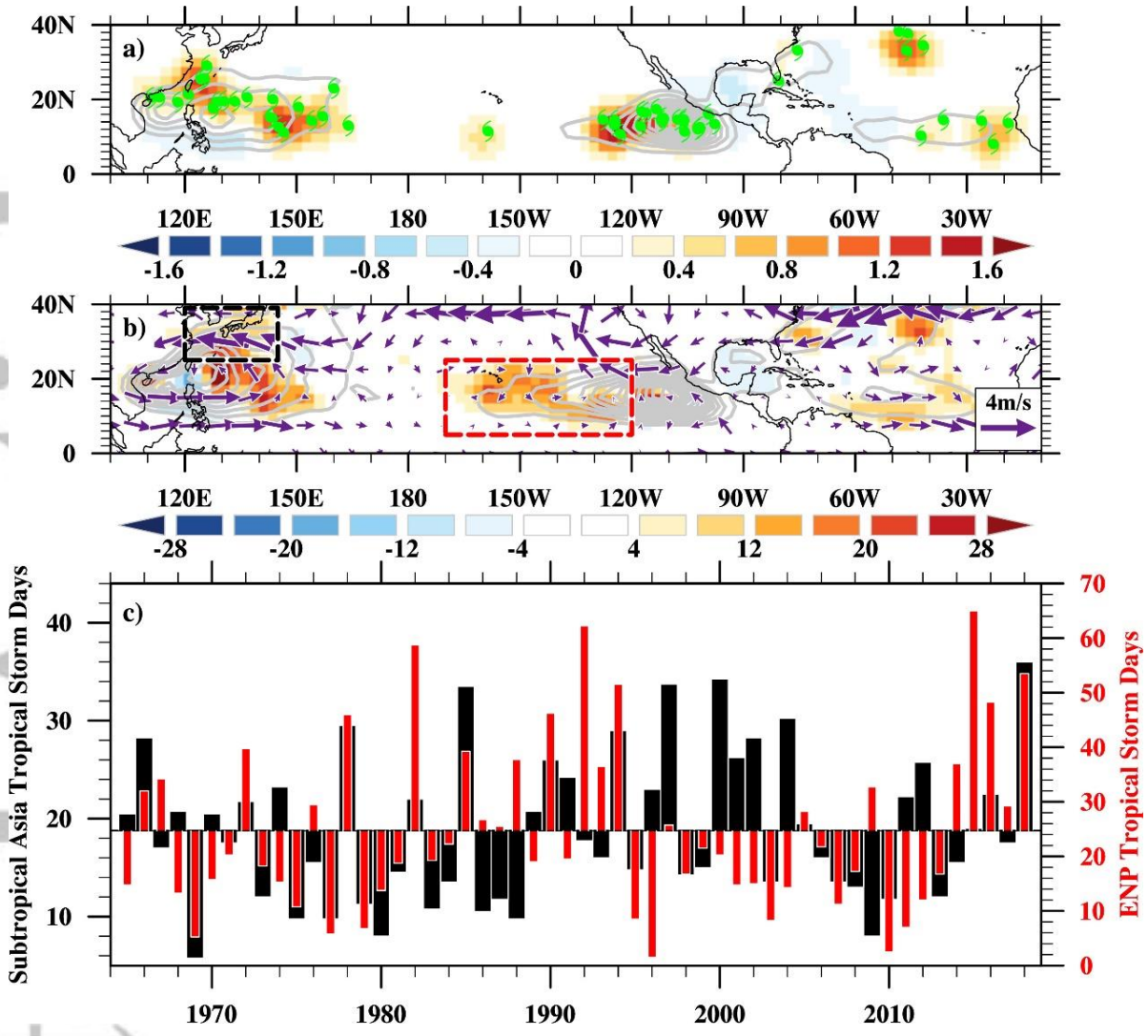

Figure 3 (a) June-September climatology (contours, occurrence year^{-1}) and anomalies (shadings, occurrence decade^{-1}) of TCG density in each 2.5°×2.5° latitude and longitude box in JJAS 2018. The green symbols represent TCG locations. (b) is same as (a) but for TC track density. The vectors denote anomalous steering flows defined as the pressure-weighted average winds from 850 to 300 hPa in JJAS 2018. (c) Time series of named storm days in subtropical Asia (black bars) and the central-eastern North Pacific (red bars) during 1965-2018. The regions of subtropical Asia and the central-eastern North Pacific are shown in (b) by the red and black box, respectively.

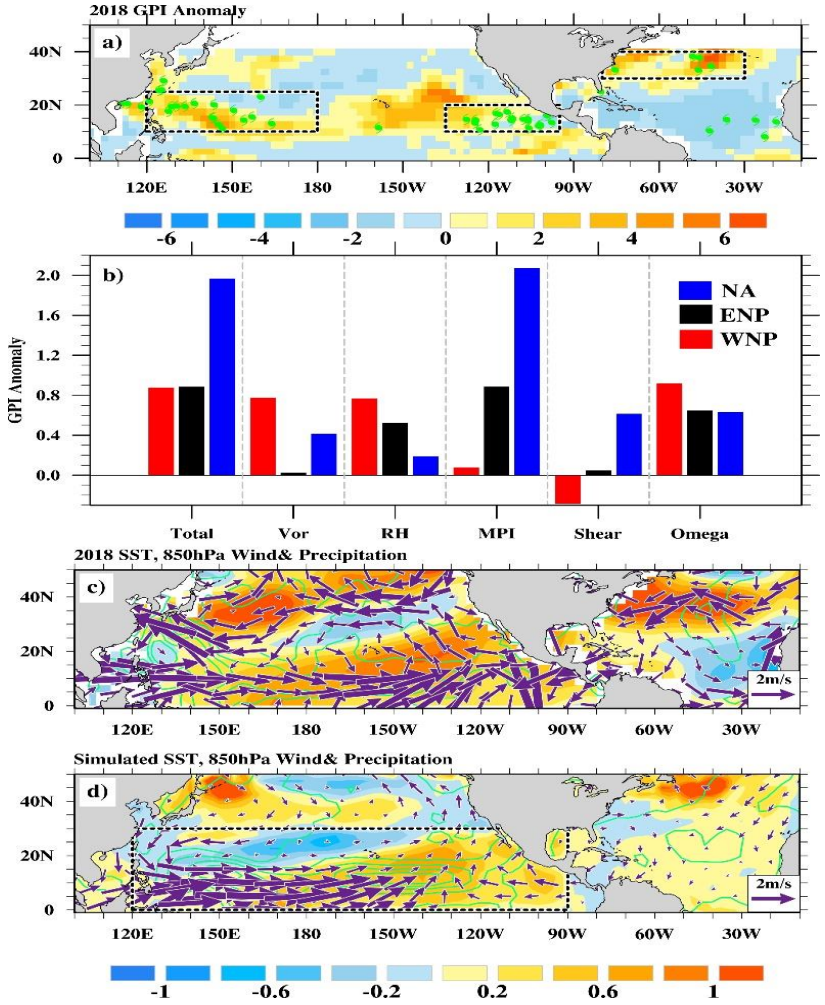

Figure 4 (a) Distribution of the normalized GPI anomalies (color shading) in JJAS 2018, (b) contributions of the five terms to the GPI anomalies in the WNP (red bars), ENP (black bars) and subtropical NA (blue bars). Vor, RH, MPI, shear and omega refers to the GPI derived from varying vorticity, relative humidity, potential intensity, vertical wind shear and omega, respectively, with other variables fixed as climatology. For the total, all five terms in the GPI are allowed to vary. (c) SST (shading, °C), 850 hPa wind (vectors, m s^{-1}) and precipitation (contours from 0 to 4 with an interval of 1, mm day^{-1}) anomalies in JJAS 2018. (d) Model simulated response of SST (shading, °C), 850 hPa wind (vectors, m s^{-1}) and precipitation (contours from 0 to 4 with an interval of 1, mm day^{-1}) anomalies to the subtropical NP SST warming. The black boxes in (a) denote the region over which GPI anomalies were calculated in the WNP, the ENP and the subtropical NA. The green symbols in (a) denote TC genesis locations in JJAS 2018. The black box in (d) indicates the regions where the SST are nudged to observation.

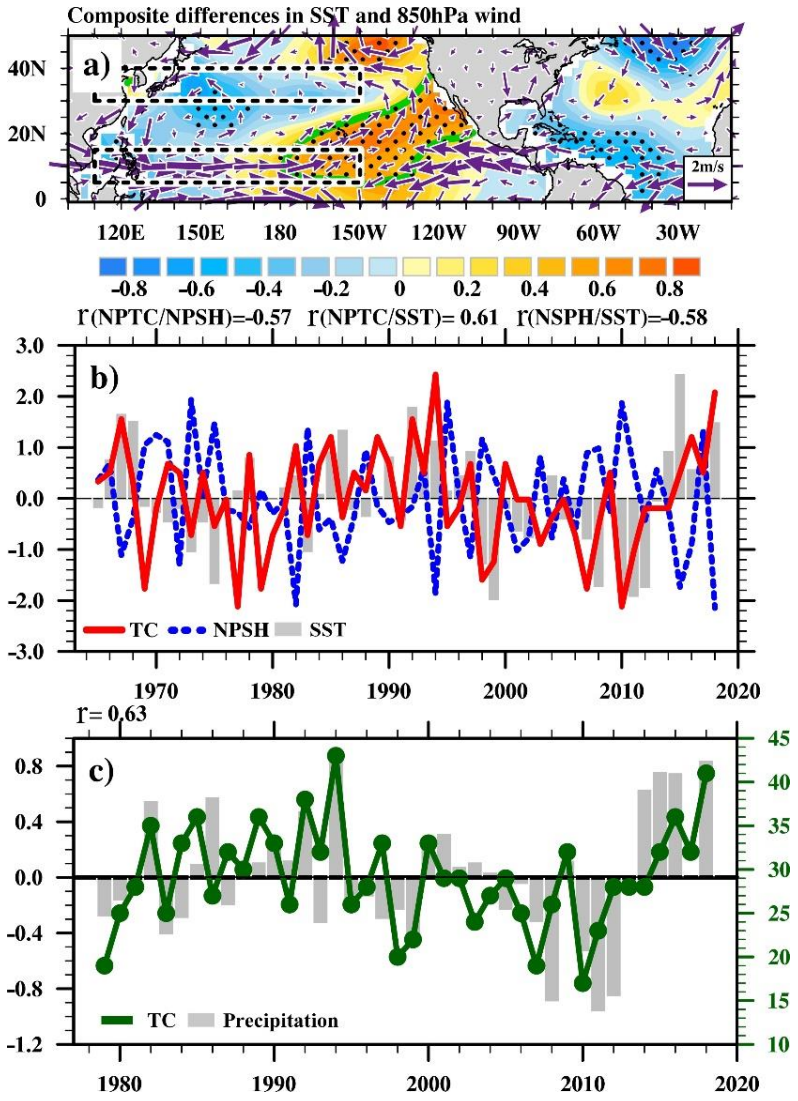

Figure 5 (a) Composite difference in JJAS mean SST (shading, °C) and 850 hPa wind (vectors, m s^{-1}) between the high and low TCG frequency years in the NP. The dots mark regions where the SST difference is significant at the 90% confidence level. The black boxes outline the defining regions of the subtropical high index, and the green line outlines the subtropical NP region. (b) Time series of the normalized JJAS mean subtropical high index (blue dashed line), subtropical NP SST (grey bars) and NP TCG frequency (red line), and their correlation coefficients (r) are shown on the top. (c) Time series of the JJAS NP TCG frequency (green dotted line) and precipitation anomaly over the subtropical NP, and the correlation coefficient (r) is shown on the top-left panel.